SPEED-GRADIENT-BASED CONTROL OF POWER NETWORK: CASE STUDY

Igor Furtat
Control of Complex Systems
ITMO University
Russia
cainenash@mail.ru

Nikita Tergoev
Electroenergetics
SPbGASU
Russia
chebeza@gmail.com

Olga Tomchina
Electroenergetics
SPbGASU
Russia
otomchina@mail.ru

Faruk Kazi
Electronics Engineering
VJTI
India
fskazi@vjti.org.in

Navdeep Singh
Electronics Engineering
VJTI
India
nmsingh59@gmail.com

Abstract
In this paper the problem of improvement of stability and performance for the power networks by means of control is addressed. An approach based on using an invariant function depending on the system variables and the speed-gradient method for control design proposed in (Pchelkina I, Fradkov A. Combined Speed-Gradient Controlled Synchronization of Multimachine Power Systems. IFAC-PapersOnLine, 2013, Vol. 46, Is. 12) is extended. The algorithm of Pchelkina and Fradkov is modified to make the control system design more flexible. Stability and performance of the closed loop system are studied for the case of the network consisting of three generators. Simulation results illustrating the system dynamics are presented.

Key words
multimachine power systems, control, stability, speed-gradient

1 Introduction

Stable synchronous behavior of power networks is important for reliable energy generation. Mathematical formulation of desirable system behavior is based on the transient stability concept introduced by J.L.Willems in 1974. Transient stability corresponds to ability of the power network to restore an appropriate steady-state after a fault, e.g., a short circuit, generator outage, line breakage, etc. [Anderson and Fouad, 1977]. The problem is to ensure that the system state remains in the basin of attraction of this (or other) equilibrium after the fault is cleared. An efficient way of maintaining stability and performance of the power networks is application of the control algorithms. A number of approaches have been developed to this problem [Pogromsky et al, 1996; Ortega et al, 2005; Guo et al, 2001]. In [Pchelkina and Fradkov, 2013] an approach based on using an invariant function (or an invariant functional), depending on the system variables for control design is proposed. The control design is based on the speed-gradient method [Fradkov, 1980].

In this paper the algorithm of [Pchelkina and Fradkov, 2013] is modified to make the control system design more flexible. Stability and performance of the closed loop system are studied for the case of the network consisting of three generators. Simulation results illustrating the system dynamics are given.

2 Design of Control Algorithm for Multimachine Power System

2.1 Model of the Controlled System

In this paper we consider the following model of the power network [Ortega et al, 2005]:

$$
\begin{aligned}
&\dot{\delta}_i(t) = \omega_i(t)\\
&\dot{\omega}_i(t) = -\tfrac{D_i}{2H_i}\omega_{Ri}(t) + \tfrac{\omega_{0i}}{2H_i}\big(P_{mi}(t) - G_{ii}E_i^2(t) -\\
&\quad -E_i(t)\sum_{j=1, j\neq i}^{n} E_j(t)\left[G_{ij}\cos\left(\delta_i(t)-\delta_j(t)\right) + \right.\\
&\quad \left. +B_{ij}\sin\left(\delta_i(t)-\delta_j(t)\right)\right]\big),\\
&T_{di}\dot{E}_I(t) = -\left[1 - B_{ii}\left(x_{di}-x'_{di}\right)\right]E_i(t) -\\
&\quad -\left(x_{di}-x'_{di}\right)\sum_{j=1, j\neq i}^{n}\left[G_{ij}\cos\left(\delta_i(t)-\delta_j(t)\right) + \right.\\
&\quad \left. +B_{ij}\sin\left(\delta_i(t)-\delta_j(t)\right)\right] + E_{fsi}(t) + u_{fi}(t),
\end{aligned}
\tag{1}
$$

where $i = 1, 2, 3$, $\delta_i(t)$ - rotor angle of the i^{th} generator, $\omega_{Ri}(t)$ - rotor angular velocity of the i^{th} generator, ω_0 - synchronous velocity, $E_{fsi}(t)$ - constant voltage,

$u_{fi}(t)$ - control signal, G_{ij}, B_{ij} - active and reactive conductivity coefficients of the i^{th} generator, x_{di}- reactances along the longitudinal axis, x'_{di} - transient reactance in the longitudinal axis, D_i - damping factor of the i^{th} generator, H_i - inertia ratio of the i^{th} generator, T_{di} - electromechanical constant of the i^{th} generator, $P_{mi}(t)$ - mechanical power input of the i^{th} generator.

The connection between the generators is described by the algebraic equations,

$$\begin{aligned}&P_{ei}(t) = P_{Ei}(t) + P_{li}(t),\\ &P_{Ei}(t) = E_i^2 G_{ii}(t) + E_i(t) \sum_{j=1, j\neq i}^{n} [G_{ij}\cos(\delta_i(t)-\\ &\quad -\ \delta_j(t)) + B_{ij}\sin(\delta_i(t)-\delta_j(t))],\end{aligned} \tag{2}$$

where $P_{Ei}(t)$ is the output electric power of the i^{th} generator, $P_{li}(t)$ is the electric power load on the i^{th} generator, $E_i(t)$ is the magnitude of the DC voltage generator to transition resistance i, G_{ii} is internal conductivity of i^{th} generator, G_{ij} is mutual conductivity between i^{th} and j^{th} generators, B_{ij} are imaginary mutual reactivities.

2.2 Speed-gradient Control Algorithm Design

Introduce the following control objective: set the initial values of the variables to provide convergence of the trajectories $\delta(t,\delta_0)$, $\omega(t,\omega_0)$, $E(t,E_0)$ to the set:

$$\begin{aligned}&0 < \delta_i < \overline{\delta} < \pi/2,\ |\omega_i| < \overline{\omega},\\ &E_i = E_{di} = \text{const} > 0,\ i = \overline{1,N}.\end{aligned} \tag{3}$$

Such an objective is related to transient stability and takes into account the network performance requirements.

To achieve control objective (3) apply the control algorithm designed by the speed gradient method [Fradkov, 1980]. Following [Pchelkina and Fradkov, 2013] assume that the internal voltage of the generator equation will have the form:

$$\dot{E}_i(t) = u_i,\ i = \overline{1,3} \tag{4}$$

where u_i are control variables.

Introduce functional V_p as follows:

$$\begin{aligned}V_p = \sum_{i=1}^{n} \Big[&\tfrac{1}{2}(E_i - E_{di})^2 +\\ &+\int_0^t \Big((E_i - E_{di} - p_i)^2 - p_i u_i\Big)d\tau\Big],\end{aligned} \tag{5}$$

where $p_i = p_i(\delta,\omega)$ C a smooth function, $z = (\delta,\omega,E)^{\text{T}} \in R^{3N}$, $E_{di} = \text{const} > 0$.

Introduce functional Q for real $V_d > 0$ such that

$$Q = |V_p - V_d|. \tag{6}$$

It uses functionality as the target, the algorithm of speed gradient:

$$\begin{aligned}&u_i = -\gamma_i \text{sign}(V_p - V_d)\cdot[E_i - E_{di} - p_i(\delta,\omega)],\\ &i = \overline{1,N}.\end{aligned} \tag{7}$$

According to the speed gradient method, one needs to evaluate the rate of change of the functional (6).

$$\begin{aligned}&\dot{Q} = \text{sign}(V_p - V_d)\cdot \dot{V}_p = \text{sign}(V_p - V_d)\times\\ &\times \sum_{i=1}^{N}\Big[(E_i - E_{di})u_i + (E_i - E_{di} - p_i)^2 - p_i u_i\Big] =\\ &= \text{sign}(V_p - V_d)\cdot \sum_{i=1}^{N}(-\gamma_i(V_p - V_d) + 1)\times\\ &\times (E_i - E_{di} - p_i)^2 \le 0,\end{aligned} \tag{8}$$

where $\gamma = \min\gamma_i > 1$. It follows from (8) that $Q(t) \geq 0$ does not increase, and hence has a limit $\lim Q(t) = Q^*$, for $t \to \infty$.

2.3 Modified Decentralized Control Algorithm

Below a modified control algorithm is described. Introduce a smooth function $p_i = p_i(\delta,\omega)$ as follows

$$p_i = \delta_i + \omega_i\mu_i - \sigma_i, \tag{9}$$

where δ_i is rotor angle of i^{th} generator, ω_i is rotor angular velocity of i^{th} generator, μ_i is normalizing factor, σ_i are some constants (design parameters) providing extra flexibility to design (the case $\sigma_i = 0$ was studied in [Pchelkina and Fradkov, 2013]).

3 Analysis of the Closed Loop Power System by Simulation

3.1 Analysis under Normal Conditions

Table 1 shows the numerical values of the parameters of the simulated power system.Each simulated generator is different from that of other mechanical power, reference level of the stator EMF, the short-circuit conductivity and thus dependent on other parameters of these values.

The results of evaluation of the control algorithm in Simulink environment in case of violation the synchronous generator mode are shown in Figure 1–2. In each figure, the following graphs are shown:

a) Rotor angle changes $\delta_i(t),\ i = 1,2,3$; rad
b) Angular velocity changes $\omega_i(t),\ i = 1,2,3$; rad/s
c) Changes of stator terminal EMF $E_i,\ i = 1,2,3$; pu.
d) Changes of the power of the transmission line to the generator $P_{Ei},\ i = 1,2,3$; pu.

As can be seen from the curves Fig. 1 Fig. 2 application developed control algorithm achieves a stable state operation of generators at the end of the transition process, regardless of the initial phase generators.

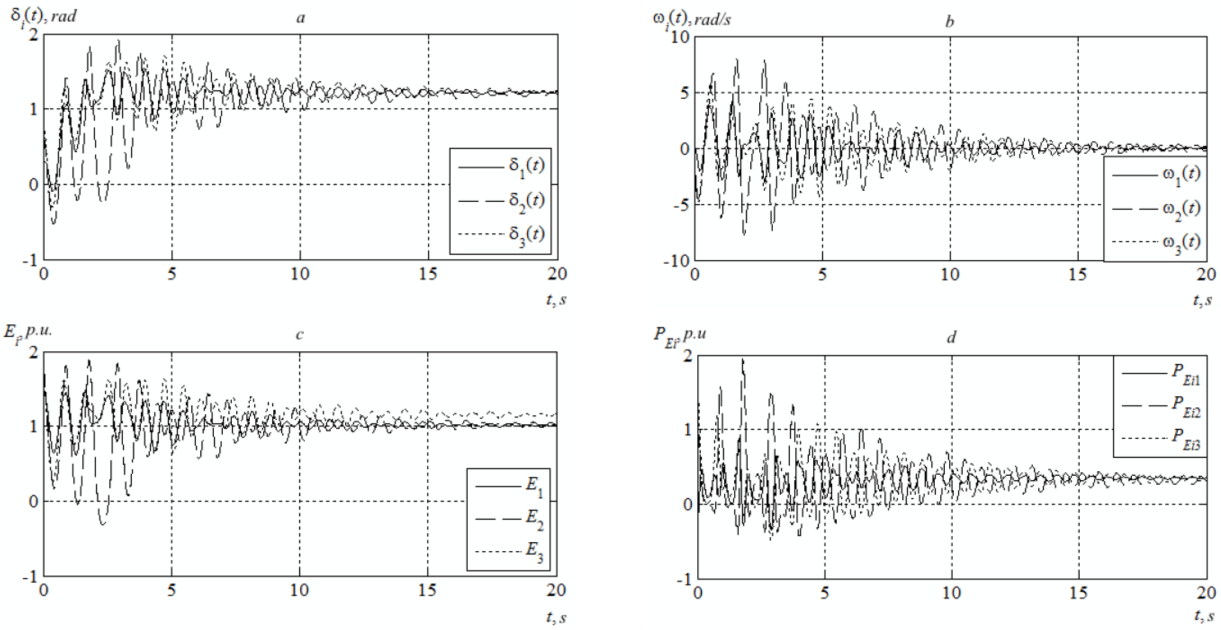

Figure 1. Transients in the network when $\delta_1(0) = \pi/10$, $\delta_2(0) = \pi/5$, $\delta_3(0) = \pi/4$.

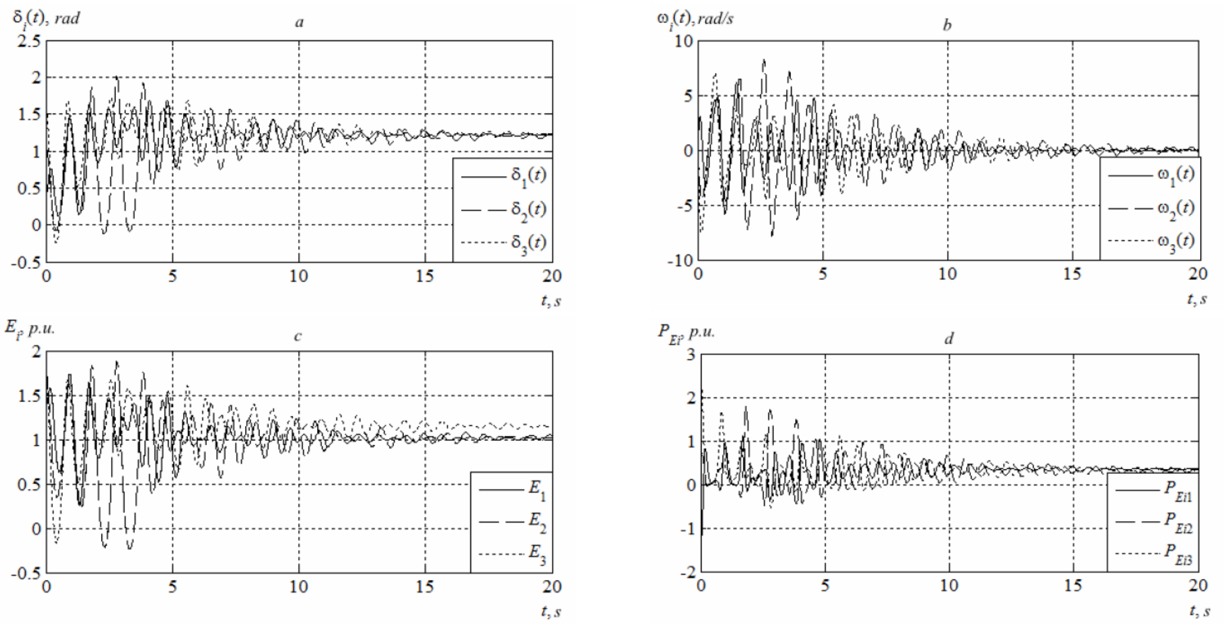

Figure 2. Transients in the network when $\delta_1(0) = \pi/8$, $\delta_2(0) = \pi/3$, $\delta_3(0) = \pi/2$.

3.2 Analysis at Breakage

In the simulation we consider abrupt change in admittance, which can be caused, for example, breakage of the transmission line between generators 1 and 2 and breakage on the lines between the first and second and first and third generator, respectively. Breakage is implemented by adding switching block to the original model (Fig. 3). Switching takes place on the line with a different conductivity from the original, and better mimics real conditions.

In the following experiments the time to switch to a backup line after the breakage occurred and the conductivity of the backup line were varied. Simulation results are shown in Table 3. Typical time histories of system variables are shown in Fig. 4, Fig. 5.

In the table the following notation is used: n is the number of lines to a breakage, $\xi = \frac{Y}{Y}$ is the ratio of the reserve to the main line conductivity, Δt is duration of the line breakage, $\max|\omega_i|$ is the maximum value of angular velocity after the reserve line, $\max\delta_i$ is the maximum value of the rotor angle ($\delta_{\text{ref}} = 72^{\text{o}} = 1.256$ rad; 20% stability margins). Note that admissible bounds for system variables are determined by Procedural Guidelines specific for each country or region. E.g. Russian document [Guidelines, 2003] stipulates that under normal power system the stability mar-

Table 3.

n	ξ, %	Δt, s	$\max\lvert\omega_i\rvert$, rad/s	$\max\delta_i$, degr.	$t_{\mathrm{tr.gen.}}$ s	$t_{\mathrm{tr.grid.}}$ s
1	60	1	0.8958	84.2	7.961	6.961
		2	0.8871	84.2	10.75	8.75
		3	0.8871	84.2	11.731	8.731
	140	1	1.2033	84.2	6.006	5.006
		2	1.3593	84.2	7.12	5.12
		3	1.4795	84.7	10.57	7.57
2	60	1	1.9018	102.3	15.036	14.036
		2	2.3522	102.3	16.771	14.771
		3	2.6519	102.3	17.748	14.748
	140	1	2.2144	102.3	8.016	7.016
		2	3.9108	102.3	12.297	10.297
		3	4.3	102.3	13.307	10.307

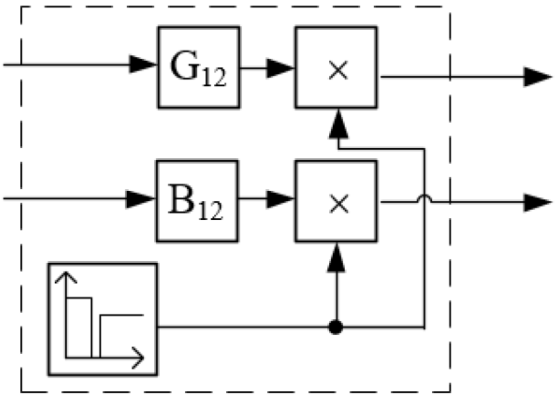

Figure 3. The structural scheme of the line breakage.

gins should correspond to the condition $K_{\mathrm{st}} \geq 20\%$, where$K_{\mathrm{st}} = \lvert\frac{\delta_i-\delta_0}{\delta_0}\rvert \cdot 100\%$, $t_{\mathrm{tr.grid}}$ is the transient time for the entire network (time from switching to the reserve line till generator rotation angles falling in the confidence interval +-5%), $t_{\mathrm{tr.gen.}}$ is the transient time for the generator (the time interval from the switching to the reserve line till entering the rotor angle into the confidence interval +-5%).

Remark: EMF of generators may be stabilized at different levels due to the different mechanical properties.

4 Conclusions

1. The algorithm ensures stable changes of generator rotor angles and angular velocities after the switch to a backup line.

2. As can be seen from Fig. 1–2 and Fig. 4–5 and table 3 with an increase in the duration of break line from 1 to 3 seconds of the transient is increased by 35% at 60% and 76% at 140% conductivity. The shorter the transmission line transients, the greater maximum values of angular velocities.

3. The maximum deviations of the rotor angles are located near the boundary of the stability phase margin at an interruption line.

4. The limited rotation angles of the rotors during a double failure when controlling off-line confirms the effectiveness of the designed algorithm, built on the principle of decentralized control.

5. In practice, the range of permissible values of the control signal depends on the desired level of energy functional, the relative rotation angles, EMF levels so that the stability region for control parameters is limited.

Future research may be aimed at the comparison of this approach with the results obtained by other methods, e.g. by [Furtat and Fradkov, 2015].

Acknowledgements

The work was supported by the Government of Russian Federation, Grant No. 074-U01 and by RFBR, grant 14-08-01015.

References

Anderson, P.M., and Fouad, A.A. (1977). *Power system control and stability*. Iowa: Iowa State University Press, 1977.

Fradkov, A.L. (1980). Speed-gradient scheme and its applications in adaptive control. Autom. Remote Control, V. 40, no. 9, pages 1333-1342.

Furtat, I.B., and Fradkov, A.L. (2015). Robust control of multi-machine power systems with compen-

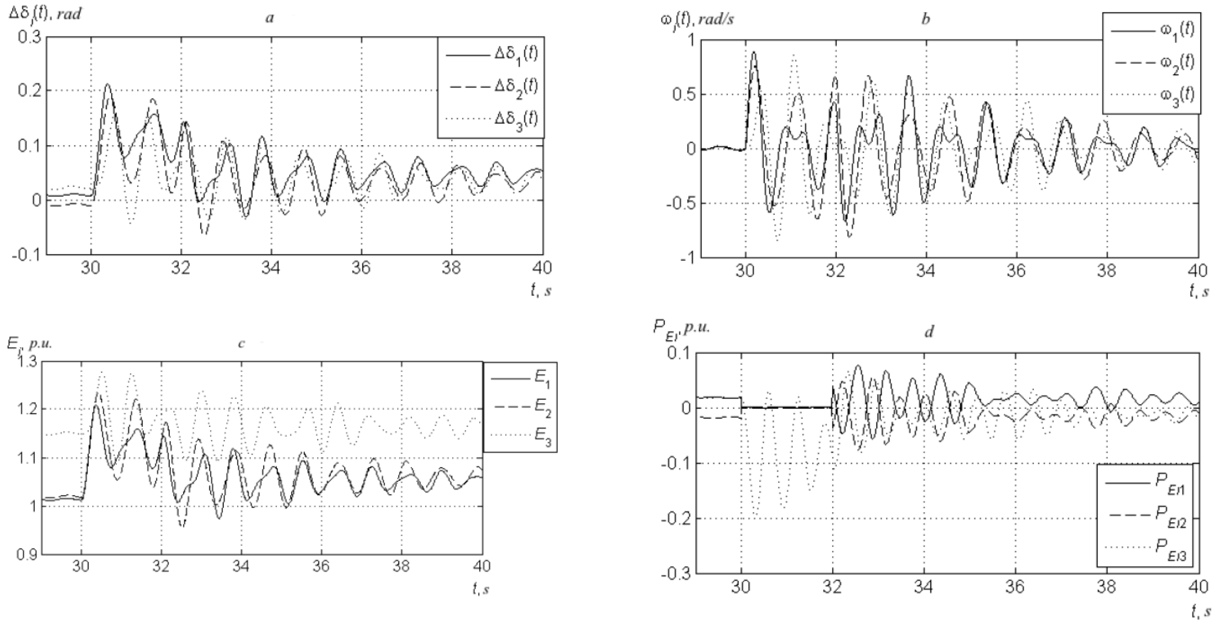

Figure 4. Simulation results for $n = 1, \xi = 60\%, \Delta t = 2$s.

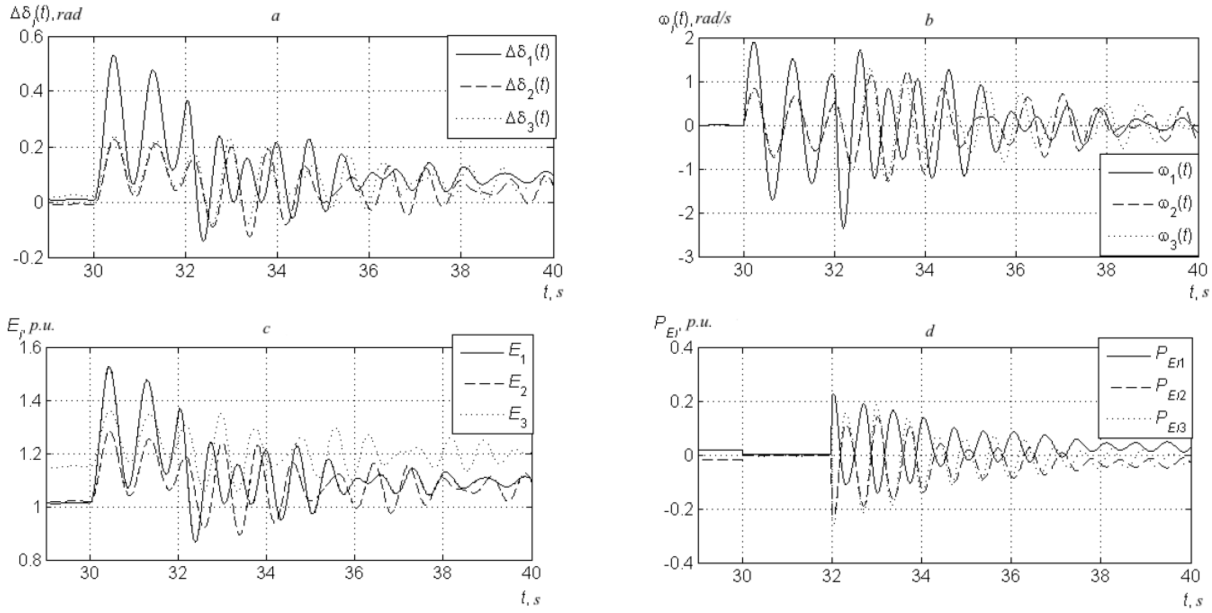

Figure 5. Simulation results for $n = 2, \xi = 60\%, \Delta t = 2$s.

sation of disturbances. International Journal of Electrical Power & Energy Systems. V. 73, Dec. pp. 584-590.

Procedural Guidelines for Stability of Energy Systems (2003). Russian Federation Minenergo, Moscow.

Guo Y., Hill, D.J., and Wang, Y. (2001). Global transient stability and voltage regulation for power systems. IEEE Trans. on Power Systems, V. 16, pp. 678-688.

Ortega, R., Galaz, M., Astolfi, A., Sun, Y., and Shen, N. (2005). Transient stabilization of multimachine power systems with nontrivial transfer conductances. IEEE Trans. on Automatic Control, V. 50(1), pp. 60–75.

Pchelkina, I., and Fradkov, A. L. (2013). Combined Speed-Gradient Controlled Synchronization of Multimachine Power Systems. IFAC-PapersOnLine, Vol. 46, Is. 12 (5th IFAC International Workshop on Periodic Control Systems. July 3-5, 2013, Caen, France, pp.59–63.)

Pogromsky, A.Yu., Fradkov, A.L., and Hill, D.J. (1996). Passivity based damping of power system oscillations // Proc. of the 35th Confer. on Decision and Control. Kobe, Japan, pp. 3876–3881.

Table 1. The values of the variables of the system

iValue	Units	1	2	3
δ_0	rad	$2\pi/10$	$2\pi/5$	$2\pi/8$
ω_0	rad s^{-1}	0	0	0
D	pu.	5	4	4
H	s	4	5	5
T_{d0}	s	1.7	2	1.9
P_m	pu.	0.9	0.8	1
E_0	pu.	1.4	1.6	1.5
E_d	pu.1.2948	1.3188		
E_f	pu.	0.1	0.1	0.1
x_d	pu.	1.863	2.17	2.01
x'_d	pu.	0.257	0.32	0.28
G_{ii}	pu.	0.5368	0.46	0.4975
$G_{12} = G_{21}$	pu.	0.1853	0.1853	—
$G_{13} = G_{31}$	pu.	0.1348	—	0.1348
$G_{23} = G_{32}$	pu.	—	0.1348	0.1348
B_{ii}	pu.	0.053	0.053	0.053
$B_{12} = B_{21}$	pu.	0.4853	0.4853	—
$B_{13} = B_{31}$	pu.	0.5348	—	0.5348
$B_{23} = B_{32}$	pu.	—	0.4853	0.4853
γ	pu.	1.3	1.5	1.3
μ	s	1	1	1
σ	rad	1.5	1.5	1.5
K_W	rad^{-1}	1	1	1

Table 2. The initial conditions for the rotor angles in the simulation

Initial conditions Figure No.	$\delta_1(0)$ rad	$\delta_2(0)$ rad	$\delta_3(0)$ rad
1	$\pi/10$	$\pi/5$	$\pi/4$
2	$\pi/8$	$\pi/3$	$\pi/2$